Lattice Numerical Simulations of Hydraulic Fractures interacting with Oblique Natural Interfaces

Elham. Bakhshi [a], Vamegh. Rasouli [b], Ahmad. Ghorbani [a, *], Mohammad. Fatehi Marji [a]

[a] *Department of Mining and Metallurgical Engineering, Yazd University, Iran*
[b] *Department of Petroleum Engineering, University of North Dakota, USA*

ABSTRACT

The hydraulic fracturing propagation is strongly influenced by the existence of natural fractures. This is a very important factor in hydraulic fracturing operations in unconventional reservoirs. Various studies have been done to consider the effect of different parameters such as stress anisotropy, toughness, angle of approach and fluid properties on interaction mechanisms including crossing, arresting and opening. Analytical solutions can only be used for simple fracture geometries and are not usually able to provide good predictions due to many simplified assumptions. Laboratory tests are also conducted under certain constraints like sample size and conditions that are different from the real field conditions. Numerical simulations, including continuum and dis-continuum based models have been used extensively to simulate hydraulic fracture propagation and its interaction with natural interfaces. However, calibration of simulated models with real field data is necessary to ensure the accuracy of the results. A calibrated numerical simulation can be used to model complex geometries. In this study, a Lattice numerical simulator, which is the advanced version of Particle flow Code (PFC) based on the granular particle physics, was used for numerical simulation of lab scale hydraulic fracturing. The scaling laws were also used to increase the dimensions of the simulated samples to allow increasing the rate of fluid injection and reducing its viscosity, hence reduce the simulation time. The interaction of hydraulic fractures and orthogonal fractures with angles of approach of 90°, 60° as well as non-orthogonal fracture planes with different filling materials ranging from strong to very weak were studied. The results showed good agreement with lab observations. In general the larger the angle of approach and stronger the filling material, the higher the likelihood of the crossing mode. Also, networks of regular natural fractures with two fracture sets were simulated. The results showed that the combination of different parameters define the preferred fracture propagation (PFP) which is not easy to predict using analytical solutions. In this situation and more complex real field cases, the use of numerical simulations are necessary to predict the propagation of hydraulic fracture and interaction modes.

Keywords : *Numerical Simulations, Lattice, Hydraulic Fracture, Orthogonal Fractures, Non- Orthogonal Interfaces, Interaction*

1. Introduction

Hydraulic fracturing is the major improved oil recovery method which is used in unconventional reservoirs. One of the main complexity in hydraulic fracturing operation in real field is due to the interaction of propagating hydraulic fracture with existing natural interfaces (e.g. natural fractures or bedding planes). This may result in failure of the intended operation. Opening, crossing, and arresting are the three interaction mechanisms proposed and studied by several researchers [1-7]. These mechanisms are function of the orientation of the induced fracture with respect to the natural fracture plane, the state of stresses, the mechanical properties of the filling material and fluid properties.

Since the 1960s, numerous experimental and analytical studies have been done to investigate the mechanism of initiation, propagation and interaction of hydraulic fracturing [8-17]. High costs and the time required to conduct the lab experimental studies and also pilot tests at field scale limit their applications. Numerical simulations, however, when correctly calibrated and cross checked with existing lab or field results, may be used effectively to run several simulations to understand the impact of different parameters in hydraulic fracture propagation and interaction modes. Several numerical models including continuum, like finite element methods (FEM) [18-22], and discontinuum, such as

discrete element methods (DEM) [23-27] have been used for simulations of hydraulic fracturing.

Displacement discontinuity method (DDM) used for modeling the extension of fracture [28, 29] and the higher order displacement discontinuity method (HODDM) using special crack tip elements has been used to study the crack propagation mechanism [30-32].

Many studies have been used particle flow code (PFC) to study the interaction mechanisms in 2D and 3D [33-37].

Lattice numerical simulation, which is a grain based model has been recently used for simulation of hydraulic fracture propagation [38, 39] and was used in this work.

In this study, XSite software [40], which works based on Lattice modelling, was used to numerically simulate the interaction of hydraulic fracture and orthogonal natural fractures with angles of approach of 90° and 60° degree, corresponding to some laboratory experiments carried out by Sarmedivaleh et al. (2014) [41]. We also extended the simulations to some non-orthogonal natural fractures as well as regular fracture network to simulate more complex and real field like cases.

2. Scaling laws

The scaling laws are used to scale the hydraulic fracturing parameters in the laboratory in order to increase these parameters. Scaling laws are

used to build a field model on the lab scale, which defines the parameters of fracturing (such as viscosity) in such a way that laboratory and field fracture propagation regimes seems similar (de Pater et al, 1994). For viscous dominated propagation regime, the dimensionless toughness parameter of a Penny-Shaped fracture can be calculated as [43]:

$$\kappa = K' \left(\frac{t^2}{\mu'^5 Q_o'^3 E'^{13}} \right)^{1/18} \quad (1)$$

Where Q_o is flow rate and t is the experiment time. In equation (1), the fracture propagation will be viscose dominated if   is below one whereas it is toughness dominated when dimensionless toughness number exceeds four.

3. Fluid/Mechanical coupling in xsite

A new coupled fluid-mechanical scheme, Mechanical Incompressible Fluid (MIF), to model the mechanisms associated with hydraulic fracturing and/or fluid injection in pre-existing fractures has been proposed by Peter Cundall and after testing it was implemented in XSite [44]. The new scheme is applicable to situations in which the rock compressibility is much larger than that of the fluid. One of the main advantages of this scheme, compared to the algorithms currently implemented in Itasca codes, is the larger (both mechanical and flow), explicit timesteps required for numerical stability. In the new scheme, a stable timestep is proportional to rock compressibility multiplied by the discretization length, which is orders of magnitude greater than the stable timestep in the current schemes, proportional to fluid compressibility multiplied by fracture aperture. The rock and fluid compressibilities are roughly of the same order of magnitude, but the fracture aperture is typically orders of magnitude smaller than the discretization length. Consider an element of rock that includes a single joint. The element has the dimension of the lattice resolution, and the joint is represented mechanically by the Smooth joint model (SJM), in which R, the unit normal vector is taken as that of the through-going joint plane rather than the normal vector linking the two associated nodes.

Fig. 1 illustrates the mechanical arrangement in the normal direction. The stiffnesses have units of force/displacement and here we consider one-dimensional stiffnesses. Thus:

$$k_F = K_F A / a \quad (2)$$

where K_F is fluid bulk modulus, A is the apparent area of the joint element (in the order of R^2, where R is the lattice resolution or discretization length) and a is the joint aperture; and

$$k_R = K_R A/a \quad (3)$$

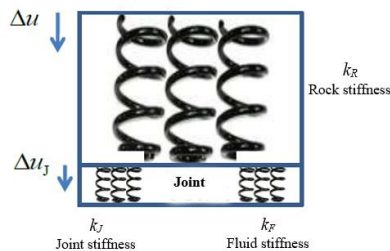where K_R is rock bulk modulus. Because R >> a typically k_F >> k_R [44].

Fig. 1. Schematic of lattice element with embedded fluid-filled joint, normal direction [44].

4. Sample preparation

In this study and for numerical simulations, the properties of the cement samples which used by Sarmadivaleh et. al (2012) [45] in their lab experiments, were used. They performed hydraulic fracturing tests on cubical samples with sides 10, 15 and 20 cm and prepared the cement mortar samples as mix of cement and water through a careful lab experimental procedure (see [45] for more details). The minimum and maximum horizontal and vertical stresses of 1000, 2000, ~3000 psi (i.e., approximately 7, 14 and 21 MPa), respectively, were applied during

testing the samples. The low fracture toughness, low permeability and low to moderate porosity are the key features that make the cement a good candidate for fracturing tests. To create artificial fracture surfaces (i.e. natural interfaces) oil coated galvanized steel sheets (2 sheets for each sample) with different sizes were placed into the mix before it sets in such a way that the sample is divided into three pieces. Artificial fractures with angles of 60°, and 90° were made on 10 and 15 cm mortar cube samples (Fig. 2). These interfaces were then glued using four different adhesives. Shear strength of these glues are listed in Table 1. Two ductile glues (Brown and Black) and two brittle ones (cement and white glue) were chosen to study the effect of interface filing material. In lack of reported friction angles for these interfaces, for the purpose of this work we considered the friction angle to be 35°, 25°, 15° and 5° for the cement, white, black and brown glues, respectively. The thickness and curing time period were kept identical for all adhesives except for the cement which needed to be cured in water.
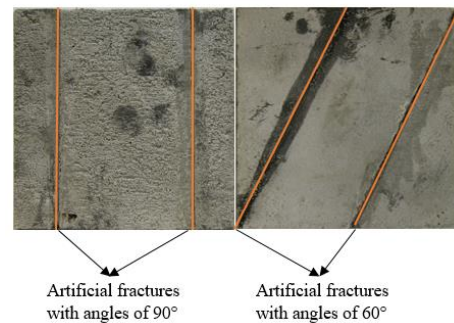

Fig. 2. Two 10 cm samples with interface of 90° (left) and 60° (right), (After [41]).

Table 1. The mechanical properties of the natural interfaces [41].

Mechanical property	Value	
Natural interface shear Strength, $_0$, psi (MPa)	Cement	290 (2)
	Brown glue	70(0.5)
	Black glue	145(1)
	White glue	3370 (26)
Natural interface friction, μ_f	0.698±0.006	

For obtaining an estimation of hydro-mechanical behavior and properties of the samples, before conducting the experiments Sarmadivaleh et, al (2012) conducted standard hydro-mechanical tests and the results of these experiments are listed in Table 2.

Table 2. The hydro-mechanical properties of the cement samples and the testing methods [41].

Hydro-mechanical property	Value	Test method
Uni-axial compressive Strength, UCS psi (MPa)	11,530 ±750 (79.5)	Unconfined compression test
Uni-axial Poisson's ratio,	0.197± 0.02	Unconfined compression test
Young's modulus, E, psi (GPa)	$4.018 \times 10^6 \pm 2 \times 10^5$ (27.74)	Unconfined compression test
Internal friction angle, (degree)	44.3	Mohr circle, confined test
Cohesion, C_c psi (MPa)	2524 (17.3)	Mohr circle, confined test
Tensile strength, T_0, psi (MPa)	510±200 (3.5)	Brazilian tensile test
Fracture toughness, K_{IC} psi √in (MPa√m)	710±200 (0.78)	CSB
Porosity, %	14.7±1	Two Boyle's cells
Permeability, K mD	0.018±0.005	Transient gas flood

Sarmadivaleh & Rasouli (2014) [41] used an injection rate of 0.1cc/min and fracturing time of 100 s in their experiments. Therefore, the dimensionless fracture toughness for fracturing fluid viscosity of 97,700 cp is calculated to be 0.47 which confirms that fracture propagation regime is viscosity dominated. Taking these parameters, the available time for the fracture to propagate within the sample before terminating the test is calculated to be around 1.5 minutes (90 seconds).

5. Simulation design parameters

The lab experiments were done by Sarmadivaleh & Rasouli (2014) [41] on 10 cm samples including two synthetically made natural interfaces. In the lab, in order to maintain the viscosity dominated fracture propagation regime, the flow rate was extremely low (1 cc/min or 1.67×10^{-8} m³/s) and the viscosity of the fracturing fluid was very high (97.7 pa.s), nearly 100,000 times larger than the viscosity of water (0.001 pa.s). Using these figures for simulations will take a very long time which may not be feasible. Therefore, here, the larger size samples were simulated, while maintaining the propagation of the fracture within the viscosity dominated regime. To do this, the size of the lab scale sample was multiplied by 50 times and cubic samples were simulated with a size of 5 m (500cm). Accordingly, among possible flow rates and viscosities, resulting in viscosity dominated regime a flow rate of 0.005 m³/s and viscosity of 0.001 pa.s were choosed for the fracturing fluid. Based on Equation (1) this will result in a value for k=0.57, which means that the fracture will propagate in viscosity dominated regime as k <1. The vertical well with a radius of 0.1m is placed in the center of the sample, and the natural interfaces were considered in the lattice model at the same location similar to the lab experiments with their properties assigned to those of cement or three glues (white, black and brown) determined in Table 1. Both natural fractures were assigned an aperture of 1×10^{-5} m. The fluid cluster with a radius of 0.25 m and a very weak starter crack is placed at the center of the wellbore with a radius of 0.30 m and aperture of 1×10^{-5} m. The starter crack is aligned in Y direction, perpendicular to the min stress, helping the induced fracture to initiate in this direction. In the lab, commonly, a notch is created along this direction to facilitate the fracture to initiate and this was practiced in the lab experiments done on the cement samples. It is important to note that the fracture aperture and pressure values within the starter crack zone do not represent the real values of the induced fracture opening and pressure as the starter crack has a much larger initial aperture than the rock matrix represented by the pipes. Therefore, the data within this zone are not included in the interpretation and are discarded from the plots. In practice, in the field, the near wellbore zone is a damaged zone and the fracture geometry and its orientation are not dictated by the far field stresses, so similar concept is used in the simulations. The magnitude of stresses were chosen as 1, 2 and 3 MPa in X,Y and Z directions.

6. Numerical simulation - Orthogonal natural interfaces

6.1. 90° Angle of Approach

The geometry of the hydraulic fracture after 1.0 s of simulation times is showed in Fig. 3. In Fig. 3 (left) the left natural fracture has white glue (very strong) properties whereas the right natural fracture has the properties of black glue (weak glue). Similarly, in Fig. 3 (right), the left and right natural fractures filled with cement and brown glue (very weak). The colors in these plots represent the fracture aperture, which is the opening of the pipes connecting the nodes in the lattice simulation after the fluid pressure reaches the failure criteria of the pipe.

From Fig. 3 it is seen that the hydraulic fracture has crossed the white glued and the cemented natural fractures. However, the extent of crossing is more manifest for the white glue fracture comparing to the cemented one.

6.2. 60° Angle of Approach

The results of lattice simulations for the cement blocks having natural interfaces with 60° angles of approach are presented in this section. Similar analyses to those conducted for simulations of samples with 90° angle of approaches were done. The fracture, similar to the previous models, propagated in penny shape before it hits the two interfaces. Fig. 4 shows the geometry of the two models with white-black and cement-brown natural fractures after 1.0 s simulation time. It is seen that the hydraulic fracture has crossed the white glued and cement interfaces but the extent of the propagation is less than in case of the 90° interface

angle models (see Fig. 3). The fracture was arrested by black and brown glued interfaces and the fluid invaded into these fractures and opened them. From field application perspective, this means that the fracturing fluid may be injected into existing faults and fractures, instead of creating an induced fracture plane.
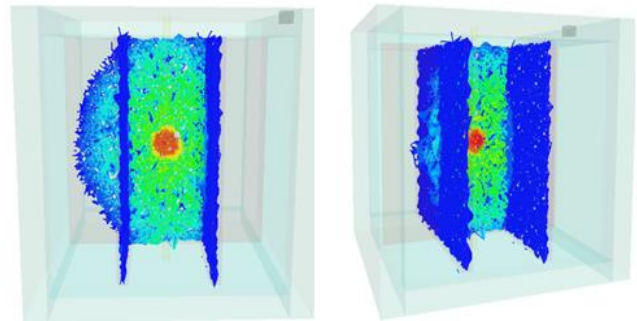

Fig. 3. Hydraulic fracture interaction simulation for 90° angle of approach. Natural interfaces filled with strong white glue and weak black glue (left) and cement and very weak brown glue (right).
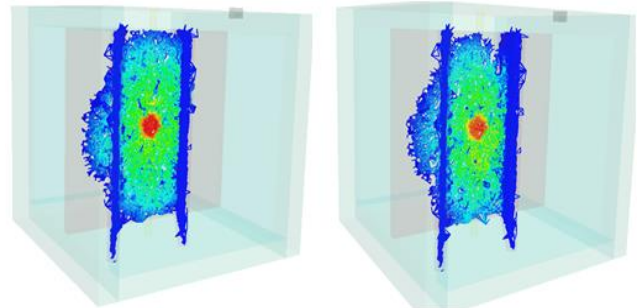

Fig. 4. Hydraulic fracture interaction simulation for 60° angle of approach. Natural interfaces filled with strong white glue and weak black glue (left) and cement and very weak brown glue (right).

7. Non-orthogonal - Natural interfaces

In section 6, simulations of natural interfaces were limited to two orthogonal planes (i.e. perpendicular to the horizontal plane) at different directions. However, in practice the planes maybe at any dip angle and orientation. Fig. 5 shows an example of two natural interfaces with dip angles of 130° (left) and 70° (right) and dip directions of 90°, respectively. The rock properties and stresses are the same as those models in the previous sections. The results of Fig. 5 show that the hydraulic fracture has crossed both strong natural fractures in this specific example.

Fig. 6 presents a different example with two non-orthogonal weak natural interfaces at different sizes. The left small size natural fracture has dip angle and dip of 130° and 90°, respectively. The orientation of the large size right natural fracture is dip angle of 70° and dip direction of 60°, respectively. This is a more common geometry that may be observed in naturally fractured reservoirs, especially in carbonate formations (Dershowitz et al, 2002). Fractures with different scales may add more complexity to the overall interaction mechanism. For example, when hydraulic fracture arrives at a weak interface with the expectation to be arrested, if the interface is of small size, the hydraulic fracture will continue its propagation when extends to the sides of the interface. This is shown in Fig. 6 (right) for the small size fracture. This figure shows how as the time evolves the hydraulic fracture may extend to the other side of the fracture. Considering several fractures with various scales, one can recognize the difficulty in predicting the preferred fracture propagation (PFP) direction. The numerical simulations can be used in this complex fracture geometry.
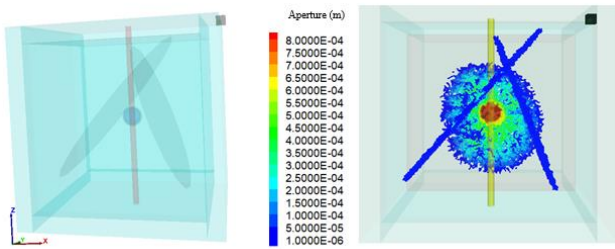
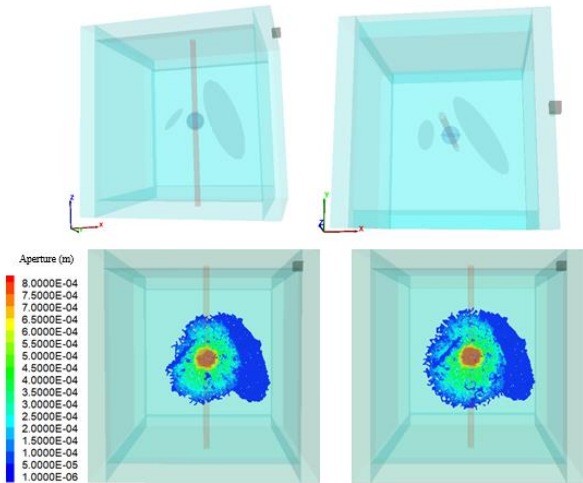**Fig. 5.** Interaction mode in case of two non-orthogonal natural interfaces.

Fig. 6. Views of the small and large sixe fractures (top) and the interaction mode in case of two non-orthogonal natural interfaces with different sizes (bottom).

8. Regular natural fracture network

In this Section, we extend the simulation to the case of two orthogonal sets of natural fractures. The geometry of the problem is shown in Fig. 7 two sets of natural fracture planes. The set parallel to X axis are very weak and the one parallel to the Y axis includes strong interfaces. The stresses are aligned 20° from X axis clockwise in order to cross the natural interfaces at an angle different than 90°. Hence, the starter crack is also in this direction to initiate the induced fracture. The Preferred Fracture Propagation (PFP) direction is shown in this Figure.
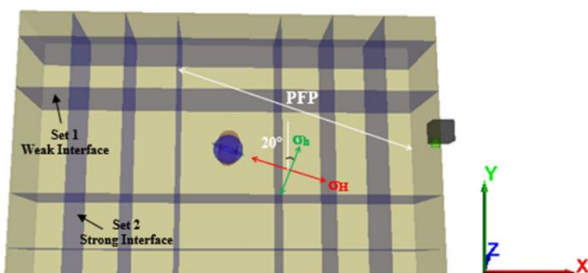

Fig. 7. Geometry of the regular fracture network.

Fig. 8 shows the results of simulations with the three principal stresses of $_v$=3 MPa, $_H$=2 MPa, and $_h$=1 MPa. The results show that the induced fracture, instead of following the PFP, has been disturbed by the existence of natural interfaces. In this example, the hydraulic fracture was unable to cross the strong interface but instead it has opened it and then entered into the weak interfaces. For comparison purposes, in Fig. 9, the model was run for isotropic horizontal stresses of 2MPa. In this case it is observed that the injected fluid will propagate more into both natural fracture sets around the wellbore due to lack of strong stress anisotropy. Changing the interface properties, as well as the state of stresses may result in any other type of response, which is impossible to

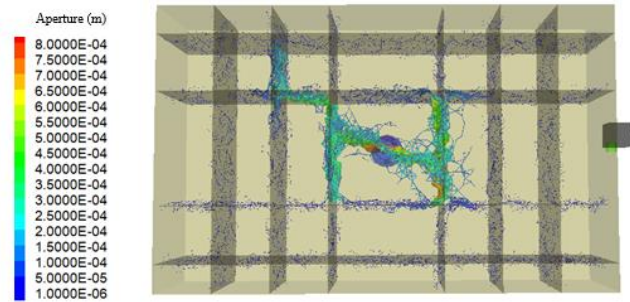predict using analytical solutions and requires the use of calibrated numerical simulations.

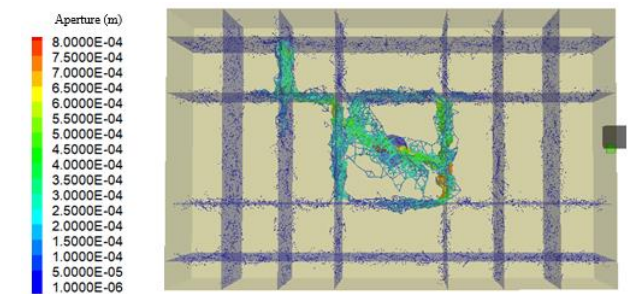**Fig. 8.** Fracture propagation when $_v$=3 MPa, $_H$=2 MPa, and $_h$=1 MPa.

Fig. 9. Fracture propagation when $_v$=3 MPa, $_H$=2 MPa, and $_h$=2 MPa.

Figs 10 and 11 show the results of the model with initial stresses of $_v$=3 MPa, $_H$=2 MPa, and $_h$=1 MPa but at two different fluid viscosities of 0.01 pa.s. and 0.1 pa.s., respectively, in comparison to Fig. 8, where the viscosity of the fluid was 0.001 pa.s. This is to investigate how the selection of the fracturing fluid may impact the operation and the geometry of the induced fracture. The results of these Figures show that as the fluid viscosity increases, the fracture has less intention to propagate further away from the wellbore and is more dispersed into the natural interfaces. In specific, in case of viscosity of 0.1 MPa, it is seen that, at the same time span, the induced fracture has propagated much less, comparing to the case of lower viscosities. These results clearly demonstrate the importance of choosing the right fluids for hydraulic fracturing operations, and the impact that the existence of natural fractures may have on interaction modes.
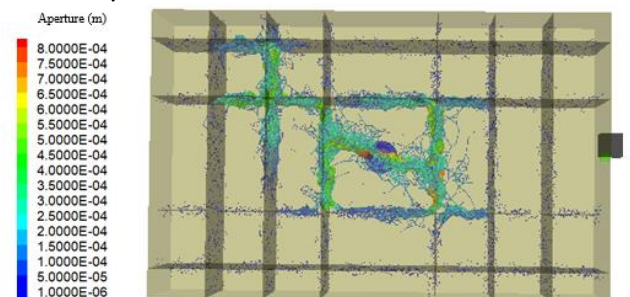

Fig. 10. Fracture propagation when =0.01 pa.s.

9. Discrete Fracture Network (DFN)

In real field application, the distribution of natural fractures is not as simple as the regular natural fractures shown in the previous section. The fractures may be at any shape and form, at different scales, and filled with different type of filling material. This implies the real complexity in predicting how the induced fracture may propagate in real field and how the combination of various parameters may affect the overall fracture initiation and propagation. Many attempts have been made to model the distribution of real natural fractures based on different statistical analysis. As described by Dershowitz et al (2002) [46] "The

DFN approach can be defined as analysis and modeling which explicitly incorporates the geometry and properties of discrete features as a central component controlling flow and transport". This approach is based on recognition of the representative elementary volume (REV), which means that at any given scale, only some of the natural fractures will contribute into the flow of the fluid and change of mechanical properties of the rock masses. This topic needs to be considered as a separate subject of research. Fig. 12 shows an example of the DFN generated through the simulations and is considered to represent presence of natural fractures in the field. Of course, the model needs to be fine-tuned after several cross check of the results with the real operations, for example, in case of hydraulic fracturing, with micro seismic data to confirm the validity of the model in predicting the PFP path.
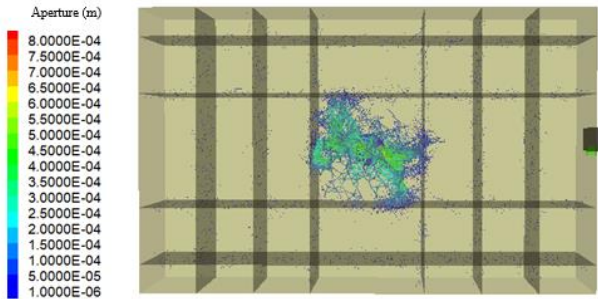

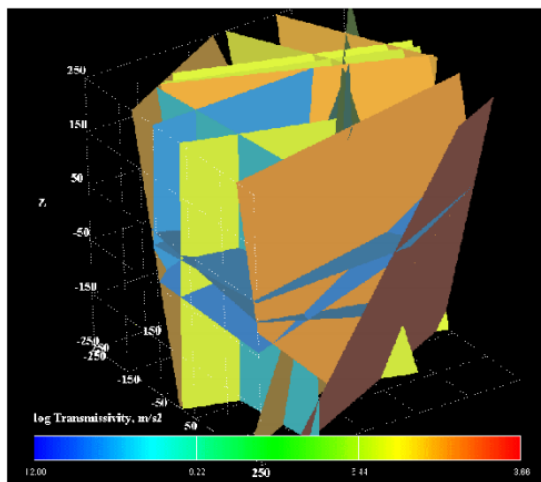**Fig. 11.** Fracture propagation when =0.1 pa.s.

Fig. 12. An example of DFN representing the natural fracture disctibution in real field (After [46]).

DFN has been successfully applied to simulate the distribution on natural fractures in Carbonates formations, where the permeability is mainly due to the second porosity, i.e. through natural fractures. The model can consider the existence of vugs, wormhole channels, and Karstic Porosity on Fracture Planes, which are common features observed in fractured carbonate reservoirs (Dershowitz et al, 2002).

10. Conclusions

Numerical simulation of hydraulic fracturing interaction with orthogonal and non-orthogonal natural interfaces were done by Lattice. For decreasing the processing time, the model size was increased. For samples with two natural fractures and two different angles of approach (i.e. 90°, 60°) with four different types of filling material, ranging from strong to very weak, hydraulic fracturing simulation was done and demonstrated that larger angle of approach and stronger interface caused increasing crossing mode.

It was concluded that in real field conditions, where combinations of different complex features (e.g. natural interfaces at different sizes and

with different properties at presence of any in-situ stresses) may exist, the use of numerical simulations is necessary to predict the hydraulic fracture propagation and the interaction modes. However, it is stressed that the numerical simulations need to be calibrated with some real field data or lab experimental observations to make sure their predictions are valid. To demonstrate the complexity in field conditions, cases with two non-orthogonal natural interfaces with different sizes and then an example of a regular natural fracture network were presented. The results indicated the complexity of predicting the FPF and the interaction mechanism when parameters are changed. The conclusion was that in real field conditions, the DFN modelling is used to simulate the distribution of natural fractures in the field and this is to be developed for simulations of hydraulic fracturing in naturally fractured formations and in particular for fractured carbonated reservoirs.

REFERENCES

[1] Murphy, H.D. and M. Fehler. (1986). Hydraulic fracturing of jointed formations. in International Meeting on Petroleum Engineering. Society of Petroleum Engineers.

[2] Warpinski, N.R. (1991). Hydraulic fracturing in tight, fissured media. Journal of Petroleum Technology, 43(02): p. 146-209.

[3] Britt, L., C. Hager, and J. Thompson. (1994). Hydraulic fracturing in a naturally fractured reservoir. in International Petroleum Conference and Exhibition of Mexico. Society of Petroleum Engineers.

[4] Jeffrey, R. and A. Settari. (1995). A comparison of hydraulic fracture field experiments, including mineback geometry data, with numerical fracture model simulations. in SPE Annual Technical Conference and Exhibition. Society of Petroleum Engineers.

[5] Branagan, P., R. Peterson, N. Warpinski and T.Wright. . (1996). Characterization of a remotely intersected set of hydraulic fractures: results of intersection well no. 1-B, GRI/DOE multi-site project. in SPE Annual Technical Conference and Exhibition. Society of Petroleum Engineers.

[6] Vinod, P., M. Flindt, R. Card and J. Mitchell. (1997). Dynamic fluid-loss studies in low-permeability formations with natural fractures. in SPE Production Operations Symposium. Society of Petroleum Engineers.

[7] Rodgerson, J.L. (2000). Impact of natural fractures in hydraulic fracturing of tight gas sands. in SPE Permian Basin Oil and Gas Recovery Conference. Society of Petroleum Engineers.

[8] Hallam, S. and N. Last. (1991). Geometry of hydraulic fractures from modestly deviated wellbores. Journal of Petroleum Technology. 43(06): p. 742-748.

[9] Behrmann, L. and J. Elbel. (1991). Effect of perforations on fracture initiation. Journal of Petroleum Technology. 43(05): p. 608-615.

[10] Halleck, P. (1994). Advances in understanding perforator penetration and flow performance, Society of Petroleum Engineers, Richardson, TX (United States).

[11] Asadi, M. and F.W. Preston. (1994). Characterization of the jet perforation crushed zone by SEM and image analysis. SPE Formation Evaluation. p. 135-139.

[12] Pucknell, J. and L. Behrmann.(1991). An investigation of the damaged zone created by perforating. in SPE Annual Technical

Conference and Exhibition. Society of Petroleum Engineers.

[13] Weijers, L., The near-wellbore geometry of hydraulic fractures initiated from horizontal and deviated wells. (1995). TU Delft, Delft University of Technology.

[14] Daneshy, A.A. (1974). Hydraulic fracture propagation in the presence of planes of weakness. in SPE European Spring Meeting. Society of Petroleum Engineers.

[15] Zhou, J., Y. Jin, and M. Chen. (2010). Experimental investigation of hydraulic fracturing in random naturally fractured blocks. International Journal of Rock Mechanics and Mining Sciences. 47(7): p. 1193-1199.

[16] El Rabaa, W. (1989). Experimental study of hydraulic fracture geometry initiated from horizontal wells. in SPE Annual Technical Conference and Exhibition. Society of Petroleum Engineers.

[17] Pursley, J.T., G.S., Penny, J.H., Benton, D.T., Greene, G.S., Nordlander, M.A., McDougall and J.W., Crafton. (2007). Field case studies of completion fluids to enhance oil and gas production in depleted unconventional reservoirs. in Rocky Mountain Oil & Gas Technology Symposium. Society of Petroleum Engineers.

[18] Chen, Z., A.P., Bunger, Xi. Zhang and R.G., Jeffrey. (2009). Cohesive zone finite element-based modeling of hydraulic fractures. Acta Mechanica Solida Sinica. 22(5): p. 443-452.

[19] Sukumar, N., N. Moës, B. Moran and T. Belytschko.(2000). Extended finite element method for three-dimensional crack modelling. International Journal for Numerical Methods in Engineering. 48(11): p. 1549-1570.

[20] Ingraffea, A. and F. H. (1980). Finite element models for rock fracture mechanics. International Journal for Numerical Methods in Engineering. 4(1).

[21] Moes, N. (1999). A Finite Element Method for Crack Growth Without Remeshing. Int. J. Numer. Methods and Eng. 46: p. 131-151.

[22] Taleghani, A.D. and J.E. Olson. (2009). Analysis of multistranded hydraulic fracture Propagation: an improved model for the interaction between induced and natural fractures. in SPE Annual Technical Conference and Exhibition. Society of Petroleum Engineers.

[23] Zhang, F., B. Damjanac, and H. Huang. (2013). Coupled discrete element modeling of fluid injection into dense granular media. Journal of Geophysical Research: Solid Earth. 118(6): p. 2703-2722.

[24] Thallak, S., L. Rothenburg, and M. Dusseault. (1991). Simulation of multiple hydraulic fractures in a discrete element system. in The 32nd US Symposium on Rock Mechanics (USRMS). American Rock Mechanics Association.

[25] Abdollahipour, A., Fatehi Marji M., Yarahmadi Bafghi, AR, Gholamnejad J. (2016). DEM simulation of confining pressure effects on crack opening displacement in hydraulic fracturing. International Journal of Mining Science and Technology.

[26] Zhao, X. and R. Young (2009). Numerical simulation of seismicity induced by hydraulic fracturing in naturally fractured reservoirs. SPE Annual Technical Conference and Exhibition, Society of Petroleum Engineers.

[27] Damjanac, B.,I. Gil,M. Pierce,M. Sanchez,A. Van As and J. McLennan (2010). A new approach to hydraulic fracturing modeling in naturally fractured reservoirs. 44th US Rock Mechanics Symposium and 5th US-Canada Rock Mechanics Symposium, American Rock Mechanics Association.

[28] Fatehi Marji, M., (2014). Numerical analysis of quasi-static crack branching in brittle solids by a modified displacement discontinuity method. International Journal of Solids and Structures. 51(9): p. 1716-1736.

[29] Fatehi Marji, M., (2015). Simulation of crack coalescence mechanism underneath single and double disc cutters by higher order displacement discontinuity method. Journal of Central South University. 22(3): p. 1045-1054.

[30] Fatehi Marji, M., H. Hosseini-Nasab, and A.H Kohsary.(2007) A new cubic element formulation of the displacement discontinuity method using three special crack tip elements for crack analysis, JP J. Solids Struct 1 (1), 61-91.

[31] Abdollahipour, A., M. Fatehi Marji, A. Yarahmadi Bafghi and J. Gholamnejad (2015). Simulating the propagation of hydraulic fractures from a circular wellbore using the Displacement Discontinuity Method. International Journal of Rock Mechanics and Mining Sciences 80: 281-291.

[32] Behnia. M., K. Goshtasbi, M. Fatehi Marji and A. Golshani. (2012). On the crack propagation modeling of hydraulic fracturing by a hybridized displacement discontinuity/boundary collocation method. Journal of Mining and Environment 2 (1).

[33] Zhou, J.,L. Zhang, A. Braun and Z. Han (2017-a). Investigation of Processes of Interaction between Hydraulic and Natural Fractures by PFC Modeling Comparing against Laboratory Experiments and Analytical Models. Energies 10(7): 1001.

[34] Zhou, J.,L. Zhang and Z. Han (2017-b). Hydraulic fracturing process by using a modified two dimensional particle flow code-method and validation. Progress in Computational Fluid Dynamics, an International Journal 17(1): 52-62.

[35] Sarmadivaleh, M., V. Rasouli and N. K. Shihab (2011-a). Hydraulic fracturing in an unconventional naturally fractured reservoir: A numerical and experimental study. The APPEA Journal 51(1): 507-518.

[36] Sarmadivaleh, M., V. Rasouli and W. Ramses (2011-b). Numerical simulations of hydraulic fracture intersecting an interbed of sandstone. Harmonising Rock Engineering and the Environment: 455.

[37] Rasouli, V., M. Sarmadivaleh and A. Nabipour (2011). Some challenges in hydraulic fracturing of tight gas reservoirs: an experimental study. The APPEA Journal 51(1): 499-506.

[38] Xing, P., Yoshioka, K., Adachi, J., El-Fayoumi, A., Damjanac, B. and Bunger, A.P. (2018). Lattice simulation of laboratory hydraulic fracture containment in layered reservoirs. Computers and Geotechnics. 100: 62-75.

[39] Bakhshi, E., Rasouli, V., Ghorbani, A. Fatehi Marji, M. Rock Mech Rock Eng (2018). https://doi.org/10.1007/s00603-018-1671-2.

[40] Itasca Consulting Group Inc., (2013). HF Simulator, Version 1.9, User's Guide.

[41] Sarmadivaleh, M., and Rasouli, V. (2014). Test design and sample preparation procedure for experimental investigation of hydraulic fracturing interaction modes. Rock Mechanics Rock Engineering. 48(1): 93-105.

[42] de Pater, C., Cleary, M., Quinn, T., Barr, D., Johnson, D. and Weijers, L. (1994). Experimental verification of dimensional analysis for hydraulic fracturing. SPE Production & Facilities. 9(04): 230-238.

[43] Detournay, E. (2004). Propagation regimes of fluid-driven fractures in impermeable rocks. International Journal of Geomechanics. 4(1): 35-45.

[44] Damjanac, B. C. Detournay,P. Cundall,M. Purvance and J. Hazzard (2011). XSite- Description of Formulation. ITASCA Consulting Group., Inc.

[45] Sarmadivaleh, M. (2012). Experimental and numerical study of interaction of a pre-existing natural interface and an induced hydraulic fracture. (Doctor of Philosophy), Curtin University.

[46] Dershowitz, W.,P. La Pointe and T. Doe (2004). Advances in discrete fracture network modeling. Proceedings of the US EPA/NGWA fractured rock conference, Portland..